Development 136, 1529-1538 (2009) doi:10.1242/dev.030098

Phosphoinositide-dependent regulation of VAN3 ARF-GAP localization and activity essential for vascular tissue continuity in plants

Satoshi Naramoto[1,2,3,†], Shinichiro Sawa[1], Koji Koizumi[1,*], Tomohiro Uemura[1], Takashi Ueda[1], Jiří Friml[3], Akihiko Nakano[1,2] and Hiroo Fukuda[1,†]

ACAP-type ARF GTPase activating proteins (ARF-GAPs) regulate multiple cellular processes, including endocytosis, secretion, phagocytosis, cell adhesion and cell migration. However, the regulation of ACAP functions by other cellular proteins is poorly understood. We have reported previously that a plant ACAP, VAN3, plays a pivotal role in plant venation continuity. Here, we report on newly identified VAN3 regulators: the CVP2 (cotyledon vascular pattern 2) 5 PTase, which is considered to degrade IP_3 and also to produce PtdIns(4)*P* from PtdIns(4,5)P_2; and a PH domain-containing protein, VAB (VAN3 binding protein). Combinational mutations of both *CVP2* and its closest homologue *CVL1* (*CVP2 like 1*) phenocopied the strong allele of *van3* mutants, showing severe vascular continuity. The phenotype of double mutants between *van3*, *cvp2* and *vab* suggested that VAN3, CVP2 and VAB function in vascular pattern formation in the same pathway. Localization analysis revealed that both CVP2 and VAB colocalize with VAN3 in the trans-Golgi network (TGN), supporting their functions in the same pathway. The subcellular localization of VAN3 was dependent on its PH domain, and mislocalization of VAN3 was induced in *cvp2* or *vab* mutants. These results suggest that CVP2 and VAB cooperatively regulate the subcellular localization of VAN3 through the interaction between its PH domain and phosphoinositides and/or inositol phosphates. In addition, PtdIns(4)*P*, to which VAN3 binds preferentially, enhanced the ARF-GAP activity of VAN3, whereas IP_3 inhibited it. These results suggest the existence of PtdIns(4)*P* and/or IP_3-dependent subcellular targeting and regulation of VAN3 ACAP activity that governs plant vascular tissue continuity.

KEY WORDS: *Arabidopsis*, VAN3, Vein, ARF-GAP, CVP2, VAB

INTRODUCTION

The trafficking of proteins by vesicle transport is essential for all eukaryotic cells. Membrane-bound transport vesicles carry cargo proteins from one compartment to another and discharge their cargoes into a specific compartment by fusing with the target membrane. ARF proteins play important roles in the recruitment of vesicle coats needed for vesicle budding and cargo selection (Donaldson and Klausner, 1994; Moss and Vaughan, 1995; Moss and Vaughan, 1998). ARF proteins function through a cycle of GTP binding and GTP hydrolysis, which leads to the GTP-bound active form and the GDP-bound inactive form of the protein. This cycle is regulated by guanine nucleotide exchange factors (GEFs) and GTPase-activating proteins (GAPs).

The ARF-GAP proteins have been categorized into three groups: ARF-GAP1 type, Git type and AZAP type in mammals (Randazzo and Hirsch, 2004). AZAPs are divided further into four subgroups based on their domain structures: ACAPs, ASAPs, AGAPs and ARAPs. Because a single ARF protein functions at multiple organelles, the intracellular site of ARF-GAP protein action is important for conferring the site specificity of ARF function. Whereas all ARF-GAP1 type proteins localize to the cis-Golgi, the AZAP-type proteins function in the post-Golgi transport pathways. For example, ACAPs and ASAPs localize to the plasma membrane (PM)/endosome (Jackson et al., 2000), AGAPs localize to the lysosome/endosome (Nie et al., 2003), and ARAPs localize to the trans-Golgi/TGN/PM (Miura et al., 2002). These results suggest that the AZAP type ARF-GAP proteins are key players in the regulation of membrane traffic in the post-Golgi transport pathways. Detailed cell biological analysis has been performed in animal cells (Jackson et al., 2000; Kam et al., 2000; Randazzo et al., 2000; Miura et al., 2002; Li et al., 2005) and these results provide a theoretical framework for understanding the molecular characterization of AZAPs in cells.

However, most of these data come from studies of cultured single animal cells. The fact that AZAPs exist only in multicellular organisms strongly suggests that AZAPs may have a variety of functions, depending on the different cell types, in multicellular organisms. Therefore, understanding the divergent roles of AZAPs in individual organisms is important. Genetic analysis with mutants of AZAPs and AZAP-related factors is one complementary approach to cultured cell-based analysis. However, no studies have reported on mutants of AZAPs in animals.

The genome of a model plant *Arabidopsis thaliana* encodes 15 ARF-GAPs, which can be classified into two groups: ARF-GAP1 and AZAP. Although animal AZAPs are differentiated functionally into ACAPs, ASAPs, AGAPs and ARAPs, *Arabidopsis* has no AZAPs other than the ACAPs, which comprise four members. We and another group have found that mutants defective in an *Arabidopsis ACAP* gene, *VAN3/SFC*, have disconnected formation of the vascular bundles in leaves (Koizumi et al., 2005; Sieburth et al., 2006). In addition, quadruple mutants of all plant ACAPs

[1]Department of Biological Sciences, Graduate School of Science, University of Tokyo, Bunkyo-ku, Tokyo 113-0033, Japan. [2]Molecular Membrane Biology Laboratory, RIKEN Advanced Science Institute, Wako, Saitama 351-0198, Japan. [3]Department of Plant Systems Biology, VIB and Department of Plant Biotechnology and Genetics, Ghent University, Technologiepark 927, 9052 Gent, Belgium.

*Present address: Department of Biology, University of Pennsylvania 415 South University Avenue, Philadelphia, PA 19104, USA
[†]Authors for correspondence (e-mails: sanar@psb.vib-ugent.be; fukuda@biol.s.u-tokyo.ac.jp)

Accepted 27 February 2009

showed an enhanced vascular phenotype of *VAN3/SFC* (Sieburth et al., 2006). These observations indicate that plant ACAPs function in the continuous formation of vascular bundles.

Plant vascular bundles comprise xylem and phloem tissues, which are generated from the procambim. In leaves, the vascular bundle, called the vein, forms a species-dependent complex network. The spatiotemporal regulation of the vascular pattern has been considered an excellent model for studying the plant developmental program. Some polarly distributed proteins were found recently to function in generating continuous vascular patterns. For example, xylogen is a glycoprotein that is secreted polarly from differentiating vascular cells towards adjacent undifferentiated cells to induce vascular differentiation and accomplish vascular connection (Motose et al., 2004). Polar auxin transport is a well-known crucial factor for continuous pattern formation of veins (Przemeck et al., 1996; Hardtke and Berleth, 1998; Mattsson et al., 1999). Many reports show a close correlation between vascular patterning and the distribution of cells with asymmetrically localized PIN proteins, which are auxin efflux carriers (Paciorek et al., 2005; Wisniewska et al., 2006). PIN proteins cycle between the endosome and the PM, and, interestingly, GNOM ARF-GEF functions in the polar exocytosis of PIN proteins (Geldner et al., 2001; Geldner et al., 2003). These results suggest that polar vesicle trafficking plays a pivotal role in the coordinated vascular pattern formation.

Because the phenotype of the *van3* mutant is largely restricted to severe vascular discontinuity, it is thought that VAN3 is a pivotal factor responsible for the vesicle transport governing the vascular continuity. Genetic interactions between *van3/sfc* and *gnom*, and between *van3/sfc* and other auxin-signaling mutants, suggest that VAN3/SFC functions in auxin transport or auxin signaling or both (Koizumi et al., 2005; Sieburth et al., 2006). Scarpella et al. (Scarpella et al., 2006) reported that subcellular PIN1 polarity in pre-procambial cells, the precursors of procambial cells, determines the route of auxin transport and the subsequent pattern of veins. In the *van3* mutant, however, PIN1 polarity is established but is not maintained in pre-procambial cells, resulting in discontinuous formation of procambial cells. These results suggest that VAN3/SFC functions in vascular continuity by regulating the polar localization of proteins such as PIN1. However, the molecular mechanism by which VAN3 regulates the polar transport of vesicles is understood poorly. We have suggested that VAN3 is localized to the TGN (Koizumi et al., 2005), which differs from the subcellular localization of animal ACAPs. This difference does not allow us to interpret VAN3 function as being simply analogous to ACAP functions in animals.

One advantage of using *Arabidopsis* as the model material is the ease of genetic analysis. Several mutants are defective in vascular continuity [e.g. *mp*, *cvp* and *fkd* (Hardtke and Berleth, 1998; Steynen and Schultz, 2003; Carland and Nelson, 2004)]. To understand the molecular function of VAN3 in vascular continuity, we searched for factors that affect VAN3 function by analyzing the genetic interactions between *van3* and mutants showing the *van3*-like phenotype. Screening proteins that interact with VAN3 has identified a dynamin, DRP1A, that functions in vascular continuity in association with VAN3 (Sawa et al., 2005). Therefore, we also rescreened VAN3-interactive proteins using the yeast two-hybrid system. The analysis of factors obtained from these approaches suggests that a specific phosphoinositide(s) plays a role in subcellular protein targeting and enhancing of VAN3 ARF-GAP activity: this information provides new insights into the upstream regulation of ACAPs.

MATERIALS AND METHODS

Plant materials and growth conditions

cvp2 and *fkd2* seeds were gifts from Nelson and Schultz. *cvl1* and *vab* seeds were obtained from the ABRC collection with stock numbers SALK 038828 (*cvl1-1*) and SALK 142575 (*vab-1*). Seeds of *cvl1-2* (SALK 070963) and *vab-2* (WiscDsLox342A08) were also used. All the mutants other than *van3-1*(L*er* background) were Columbia background. Surface-sterilized seeds were plated on growth medium containing Murashige and Skoog basal salts, 1.0% (w/v) sucrose, 0.05% (w/v) Mes (pH 5.7) and 0.8% (w/v) Bact Agar (Becton Dickinson).

Establishment of the transgenic plants expressing fluorescence tagged full length and mutated forms of VAN3

The 3×[$(Gly)_3$Ser]-VENUS sequence was amplified by PCR from the pCS2 plasmid (Nagai et al., 2002). The *VAN3-VENUS* construct was made using a TT-PCR method (Tian et al., 2004) with the 3×[$(Gly)_3$Ser]-VENUS sequence and the 8.6 kb *Xba*I-*Spe*I genomic fragment of *VAN3* that contained the 1.1 kb upstream and the 1.1 kb downstream, as templates. The VAN3-VENUS fragment was cloned into pCAMBIA1300 at *Xba*I and *Spe*I sites, resulting in VAN3-VENUS translational fusion. For construction of VAN3 derivatives, essentially the same procedure was used. For subcellular localization analysis of VAN3, transgenic plants harboring VAN3-VENUS were crossed with lines expressing ST-sGFP, sGFP-SYP41 and sGFP-ARA7/RAB-F2b (Wee et al., 1998; Uemura et al., 2004; Goh et al., 2007), which had been developed by ourselves. For observing the signals of sGFP and VENUS, Zeiss LSM 510 META system was used. sGFP (Niwa et al., 1999) and VENUS were excited with 488 nm line of Argon laser and emitted fluorescence was detected with META detector from 505 to 580 nm. The reference for sGFP or VENUS was obtained from cells expressing only the sGFP or VENUS fused protein. We also obtained the reference for autofluoresence (background) from non-transformed cells. Based on these references, sGFP and Venus signals were separated by Emission Fingerprinting.

Agrobacterium-mediated transient expression of genes

The genomic fragment of *VAB* and the cDNA fragment of CVP2 were cloned into a binary vector containing YFP: pH35GY (Kubo et al., 2005). VAN3cDNA was cloned into a binary vector containing GFP: pGWB2 (Nakagawa et al., 2007). These DNA fragments were introduced into leaves of *Nicotiana benthamiana* with *Agrobacterium tumefaciens* GV3101 (pMP90). Segregation of the fluorescent signals between sGFP and VENUS was performed as described above.

Whole-mount immunolocalization

Whole-mount immunolocalization of PIN1 was performed with anti-PIN1 (1:1000) and Cy3-conjugated anti-rabbit secondary antibodies (1:600) as described by Friml et al. (Friml et al., 2003).

Split-YFP assay

cDNA fragments of *VAN3*, *VAL3* and *VAB* were used for the split-YFP assay. The YFP was split between residues 154 and 155 into nYFP and cYFP parts (Bracha-Drori et al., 2004; Walter et al., 2004). The chimeric gene was subcloned under the control of 35S promoter and the NOS terminator. Co-introduction of *VAN3-nYFP* or *VAL3-nYFP* with *VAB-cYFP* into protoplasts from *Arabidopsis* cultured cells was performed as described previously (Koizumi et al., 2005).

Yeast two-hybrid assay

The yeast two-hybrid assay was carried out as described previously (Sawa et al., 2005). The cDNAs for *VAN3* and *VAB* were subcloned into pENTR D-topo (Invitrogen) and then moved into pAD-GAL4-GWRFC and pBD-GAL4-GWRFC (Sakai et al., 2008). Plasmids containing *VAN3* and *VAB* were introduced into AH109 strain (Clontech).

Expression and purification of GST-tagged VAN3 and myristoylated AtARF1

DNA for VAN3, $VAN3^{G321E}$ and the GAP-ANK domain of VAN3 was amplified by RT-PCR. These DNA fragments were cloned into the pGEX6p-1 vector and expressed in *Escherichia coli* BL21 (DE3). The cells expressing the fusion proteins were resuspended in lysis buffer [50 mM Tris (pH 8.0),

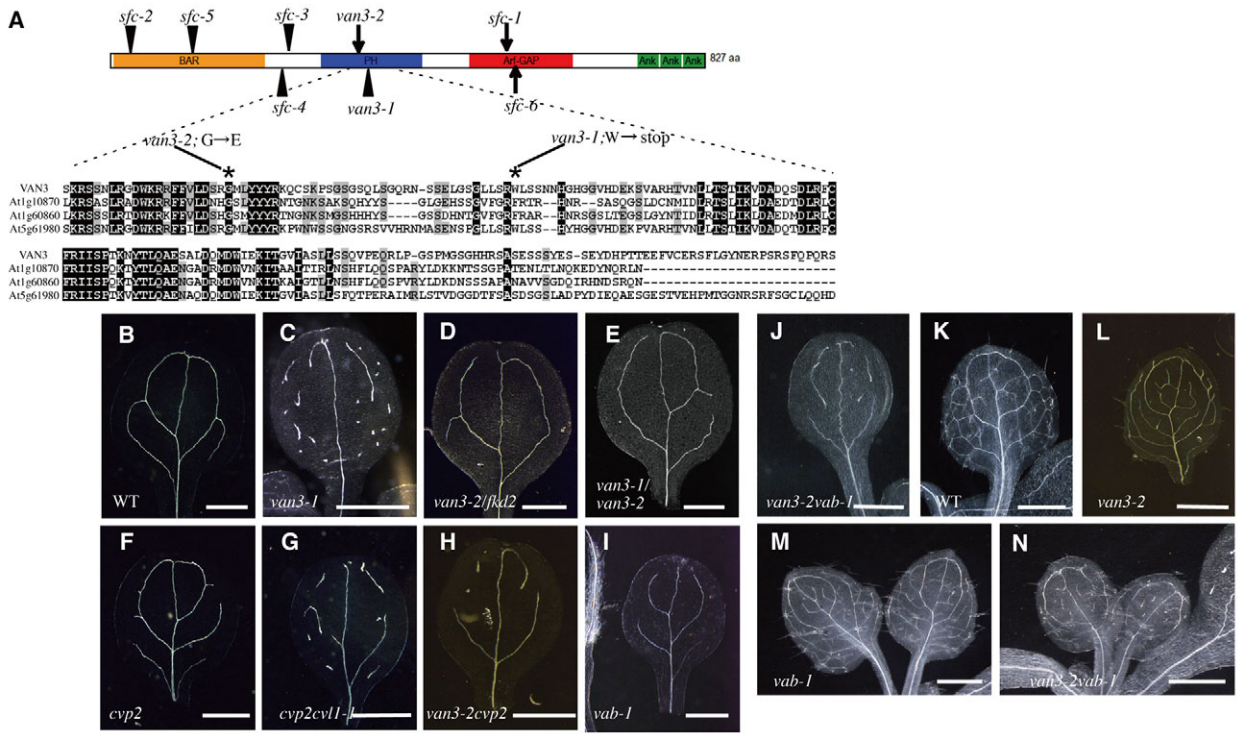

Fig. 1. Illustration of the positions of *VAN3* mutations and the venation patterns of *van3*-related mutants. (**A**) Diagram of the *VAN3* gene structure and the alignment of sequences of the PH domain of VAN3 and its homologues. Arrowheads indicate nonsense, frameshift or deletion mutations that lead to a strong *van3* phenotype. Arrows indicate missense mutations. (**B-J**) Vein patterns of cotyledons. Wild type (B), a *van3-1* mutant (C), a *van3-2* mutant (D), a *van3-1/van3-2* mutant (E), a *cvp2* mutant (F), a *cvp2cvl1* mutant (G), a *van3-2cvp2* mutant (H), a *vab* mutant (I) and a *van3-2vab* mutant (J). (**K-N**) Vein patterns of first leaves. Wild type (K), a *van3-2* mutant (L), a *vab* mutant (M) and a *van3-2vab* mutant (N). Scale bars: 1 mm.

150 mM NaCl, 0.1% mercaptoethanol and protease inhibitor cocktail (GE Healthcare)] and sonicated. Cell extracts were centrifuged at 10,000 ***g*** for 30 minutes, and the supernatant was loaded onto a glutathione-Sepharose 4B column (GE Healthcare). After washing with 10 column volumes of buffer [50 mM Tris (pH 8.0), 500 mM NaCl and 0.1% mercaptoethanol], GST-VAN3 was eluted with elution buffer [20 mM reduced glutathione, 50 mM Tris (pH 8.0), 150 mM NaCl, and 0.1% mercaptoethanol]. Myristoylated AtARF1 was purified from *Escherichia coli* BL21 (DE3) that was co-transfected with expression vectors for AtARF1 and yeast *N*-myristoyltransferase, as described previously (Koizumi et al., 2005).

ARF-GAP activity assay

Nucleotide exchange in the myristoylated AtARF1 was measured by monitoring the change in autofluorescence from intrinsic Trp. The purified myristoylated AtARF1 protein (0.5 μM) was preloaded with 40 μM GTP in reaction buffer (50 mM HEPES, 2 mM EDTA, 1 mM $MgCl_2$, 1 mM DTT and 100 mM NaCl) for 10 minutes, and 3 mM $MgCl_2$ was added to stop the GTP-loading reaction. GTP hydrolysis was initiated by the addition of GST, GST-VAN3 or GST-GAP-ANK with the indicated phospholipids. The fluorescence shift was detected with a fluorescence spectrophotometer (F-2500; Hitachi High Technologies) at an excitation wavelength of 298 nm and an emission wavelength of 340 nm.

Primer information

Primer details can be provided on request.

RESULTS

Identification of a new allele of *van3*

Previously isolated *van3/sfc* alleles display various strength of defect in the continuity of the leaf vasculature and its phenotype was not significantly affected by the ecotype (Deyholos et al., 2000; Koizumi et al., 2000; Koizumi et al., 2005; Sieburth et al., 2006). Many of these alleles carry a nonsense or frameshift mutation before the catalytic ARF-GAP domain, whereas a few missense mutations such as *sfc-1* and *sfc-6* are mapped onto the ARF-GAP domain. However, no missense mutation in other domains of VAN3 was identified (Fig. 1A). *fkd2* has a defect in the venation pattern (Fig. 1B,D) and its mutation has been mapped close to the *VAN3* locus (Steynen and Schultz, 2003). Complementation test between these genes demonstrate that *fkd2* was not rescued by *van3-1*, and its phenotype was dominant over the strong *van3* phenotype (Fig. 1C-E), indicating that *FKD2* reduces VAN3 function. Sequencing of *fkd2* revealed a point mutation from G to A, which resulted in the change of amino acid from G to E in the PH domain of VAN3 (Fig. 1A). We concluded that *fkd2* is an allele of *van3*, and we named *fkd2* as *van3-2*. These results suggest that the PH domain is necessary for VAN3 function to connect the leaf vascular cells.

Subcellular localization of VAN3 in planta

We have reported from studies of the transient expression of VAN3-VENUS that VAN3 may localize both to subpopulations of the TGN and to unknown organelles in *Arabidopsis* suspension cells (Koizumi et al., 2005). Here, we re-examined the in situ localization of VAN3 using *van3-1* mutant lines that had been rescued by *pVAN3::VAN3-VENUS* (Fig. 2A). To identify the subcellular localization of VAN3-VENUS, we introduced GFP tagged-organelle marker genes into the VAN3-VENUS plants by crossing.

The fluorescent signal of VAN3-VENUS showed dot-like localization in leaf vascular cells (see Fig. S1A-C in the supplementary material). This dot-like localization of VAN3-

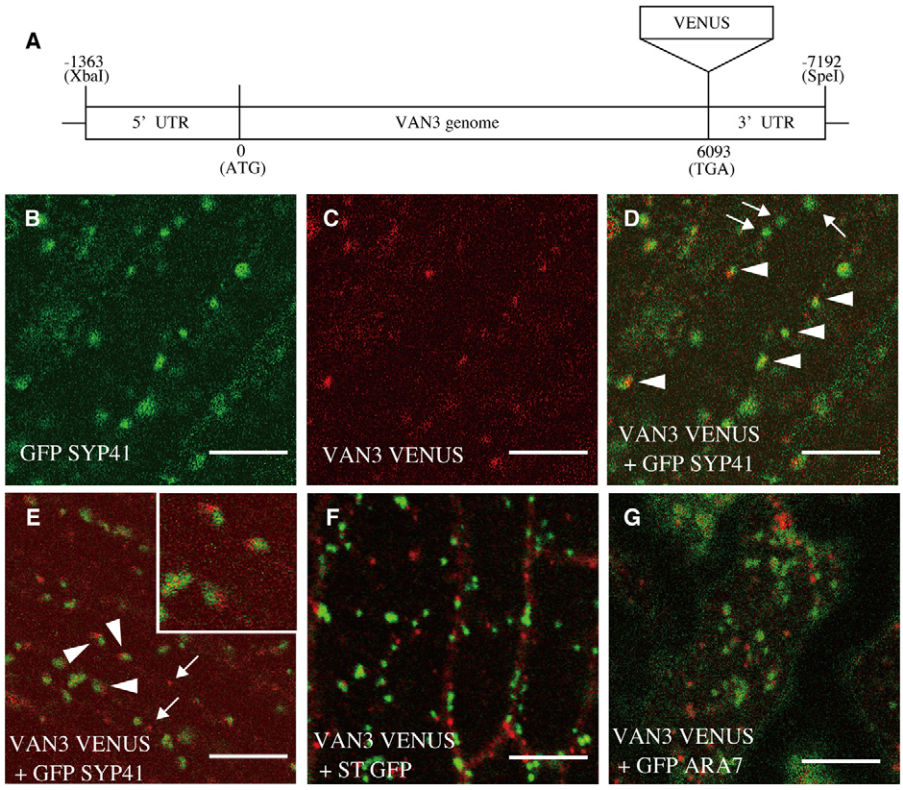

Fig. 2. Subcellular localization of VAN3. (**A**) Overview of the functional VAN3-VENUS fusion construct used. The positions indicated are relative to the translational start site. The VENUS tag was translationally fused to the 3′ end of the ORF of the genomic *Xba*I-*Spe*I fragment. (**B-G**) Localization of GFP-tagged organelle markers (green) and VENUS-tagged VAN3 (red) in young leaf petioles. Localization of the TGN marker GFP-SYP41 (B), VAN3-VENUS (C) and their merged image (D). Merged images of VAN3-VENUS with GFP-SYP41 (E), with the Golgi body marker ST-GFP (F) and with the PVC marker GFP-ARA7/RAB-F2b (G). The inset of E indicates an enlarged view of the TGN-localized VAN3-VENUS. The arrowheads show the TGN-localized VAN3-VENUS and the arrows show the VAN3-VENUS signal that is not marked by GFP-SYP41. Scale bars: 10 μm.

VENUS was observed in all tissues, including immature leaves, petioles and the root stele, in which VAN3 was expressed (see Fig. S2 in the supplementary material). This result indicates that the dot-like localization of VAN3 is common feature in VAN3-expressing cells. Next, we investigated colocalization of the VAN3-VENUS and various organelle markers. Because signals from leaf vascular cells were too weak to determine reliable colocalization with leaf vascular cells, we used petiole cells and root vascular cells in which enough fluorescence signals could be obtained. Dot-like fluorescence of VAN3-VENUS colocalized with some but not all fluorescence signals of the TGN marker GFP-SYP41 (Uemura et al., 2004) (Fig. 2B-E). VAN3-VENUS did not colocalize with the Golgi body marker ST-GFP (Wee et al., 1998) (Fig. 2F) or with the PVC marker GFP-ARA7/RAB-F2b (Goh et al., 2007) (Fig. 2G). As in the subcellular localization of the VAN3-VENUS in *Arabidopsis* suspension cells, VAN3-VENUS also localized to organelles that were not recognized by known organelle markers (Fig. 2D,E, arrows). These results clearly indicate that VAN3 resides both in a subpopulation of the TGN and in unknown organelles. Interestingly, VAN3-VENUS was not distributed uniformly but formed discriminate domains in the TGN marked by GFP-SYP41 (Fig. 2D,E, arrowheads). This result suggests that the TGN segregates into distinct membrane domains that display different biochemical compositions.

Next, we analyzed the requirement of each domain of the VAN3 protein for its proper localization. We generated a series of truncated VAN3 proteins fused to the N terminus of sGFP and expressed them under the authentic promoter in plants. Fig. 3A includes a schematic representation of VAN3-sGFP fusion proteins. Transgenic plants expressing BAR-PH-GAP-sGFP or BAR-PH-sGFP showed dot-like fluorescence signals (Fig. 3B,C), which were similar to those in the full-length VAN3-VENUS (Fig. 2C). By contrast, the BAR-sGFP lines resulted in nuclear and cytoplasmic localization of the fluorescence (Fig. 3D). Deletion of the BAR domain also caused the cytoplasmic localization of the fluorescence (Fig. 3E-H). These results suggest that both the BAR and the PH domains are essential for the proper localization of VAN3.

Role of At5PTase for maintaining vascular continuity

We have reported that the PH domain of VAN3 binds preferentially to PtdIns(4)*P* (Koizumi et al., 2005). PtdIns(4)*P* is produced by the phosphorylation of PI and the dephosphorylation of PtdIns(4,5)P_2 through the action of PI4 kinases and inositol 5′ phosphatases, respectively. *CVP2*, which encodes an inositol polyphosphate 5′ phosphatase (At5PTase), may function in the VAN3-related signaling pathway because of the phenotypic similarity between *cvp2* and *van3-2* mutants (Carland et al., 1999; Carland and Nelson, 2004). Therefore, we analyzed the genetic interaction of *CVP2* and *VAN3* in terms of vascular continuity.

Vascular discontinuity caused by the *cvp2* mutation was restricted in the marginal region of cotyledons and leaves (Fig. 1F), whereas *van3-1* caused many vascular islands (VIs) in leaves (Fig. 1C). We presumed that this difference is due to the presence of a redundant paralogue of *CVP2*. Search of the *Arabidopsis* genomic database showed a candidate of the paralogue, *At2g32010*, which was named *CVL1* (*CVP2*-like gene). *CVL1* encodes a protein comprising 582 amino acids, of which 459 amino acids were identical to those of CVP2. Although *cvl1-1* and *cvl1-2* single mutants did not cause any vascular defect (data not shown), the *cvp2cvl1-1* double mutant showed an enhanced phenotype of *cvp2* (Fig. 1G), which is reminiscent of *van3-1* (Fig. 1C). The same result was also obtained by using *cvl1-2* allele (data not shown). These results suggest that both *CVP2* and *CVL1* function redundantly in the continuity of veins, although *CVP2* is predominant.

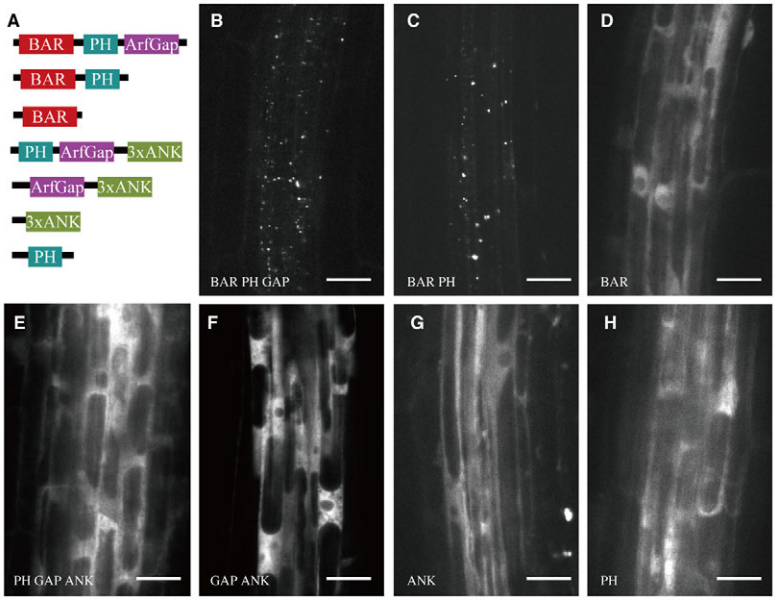

Fig. 3. The involvement of the BAR and PH domain in the subcellular localization of VAN3. (**A**) Schematic representation of deletion mutant proteins of VAN3. (**B-H**) Confocal images of the root vascular cells expressing sGFP-tagged VAN3 deletion mutant proteins under the control of the authentic promoter. BAR-PH-ARFGAP-sGFP (B), BAR-PH-sGFP (C), BAR-sGFP (D), PH-ARFGAP-3×ANK-sGFP (E), ARFGAP-3×ANK-sGFP (F), 3×ANK-sGFP (G), and PH-sGFP (H). Scale bars: 50 μm.

Judging from the number of VIs, the phenotype of *van3-2* was enhanced by introducing the *cvp2* mutation (Fig. 1D,H), whereas the phenotype of *van3-1* was not affected by the *cvp2* mutation (data not shown). Genetic analysis of triple mutants between *sfc-9*, *cvp2* and *cvl1-1* also identified that the strength of vascular phenotype was essentially the same as *sfc-9* (see Fig. S3A-C in the supplementary material). It has recently been reported that VAN3 is involved in the maintenance of continuous PIN1 expression domains in leaf primodia (Scarpella et al., 2006). To investigate whether CVP2/CVL1 is also involved in this process, we performed PIN1 antibody staining in leaf primodia. Similar to the result obtained by Scarpella et al. (Scarpella et al., 2006), in *sfc-9*, files of cells expressing PIN1 were first produced continuously and then became discontinuous during leaf development, showing a defect of the maintenance of continuous PIN1 expression (see Fig. S4M-P in the supplementary material). *cvp2cvl1-1* showed the same defect in maintenance of continuous PIN1 expression (see Fig. S4D-H in the supplementary material) and the PIN1 expression pattern of *sfc-9cvp2cvl1-1* was essentially the same as that of *sfc-9* and *cvp2cvl1-1* (see Fig. S4Q-T in the supplementary material). These results suggest that VAN3 and CVP2/CVL1 act on the pathway at the same point to regulate the continuity of the leaf vasculature.

To analyze the link between VAN3 and CVP2 further, these two proteins were fused to sGFP and eYFP, respectively, and co-expressed in tobacco leaf epidermal cells by *Agrobacterium*-mediated transformation. They colocalized significantly to the dot-like structures (Fig. 4A-C). We also confirmed the functionality of CVP2-eYFP by introducing *pCVP2::CVP2-GFP* in *cvp2* mutants (data not shown). These results further strengthened the connection between VAN3 and CVP2.

CVP2-dependent subcellular localization of VAN3

VAN3 binds preferentially to PtdIns(4)*P*, a possible product of CVP2, presumably through its PH domain (Koizumi et al., 2005). The PH domain also binds to soluble IP_3 [Ins(1,4,5)P_3], which is hydrolyzed by CVP2. Therefore, CVP2 may affect VAN3 function by regulating the cellular levels of PtdIns(4)*P* and/or IP_3. Because the PH domain is related to the subcellular localization of proteins, we examined whether *CVP2* mutation would affect the subcellular localization of VAN3. At first, we observed the localization of VAN3-sGFP in the leaf vasculatures of *cvp2cvl1-1* mutants. Although it was difficult to focus on detail because of the weak fluorescence of VAN3-sGFP, it seems that localization of VAN3 is disturbed in *cvp2cvl1-1* mutants (see Fig. S1D,E in the supplementary material). To clarify this issue, we performed subcellular localization analysis using the root vascular cells that give us reliable signals. In *cvp2* mutants, dot-like structures derived from sGFP-tagged VAN3 was not largely different from wild-type background (Fig. 4D,E). By contrast, combinational mutations between *CVP2* and *CVL1* induced the mis-location of VAN3-sGFP from dot-like structures to the cytoplasm (Fig. 4F). To explore the cooperation of VAN3 and CVP2 further, we used a translational product of *van3-2* ($VAN3^{G321E}$), which has a mutation within the PH domain. Subcellular localization of $VAN3^{G321E}$-sGFP mutants changed dramatically from the dot-like to cytoplasmic localization, accompanied by few dot-like structures in *cvp2* (Fig. 4H), but essentially the same in the wild type (Fig. 4G). These results clearly indicate that functional CVP2 or CVL1 is necessary for localization of VAN3 onto the TGN membranes.

Identification of new player function in phosphoinositide signaling-mediated vascular continuity

To isolate the new player acting on vascular continuity through VAN3-mediated phosphoinositide signaling, we performed a yeast two-hybrid screening and obtained At3g63300 as a candidate. We confirmed its interaction by the yeast two-hybrid assay (see Fig. S5 in the supplementary material) and named it as a VAN3-binding protein (VAB), which possessed a PH domain and an unknown domain, DUF828 (Fig. 5A,B).

To determine whether VAB is associated with VAN3 in situ, we first examined the colocalization of VAB and VAN3 by transient co-expression of VAB-eYFP and VAN3-sGFP in *Nicotiana benthamiana* leaf epidermis. In epidermal cells, VAB-eYFP and VAN3-sGFP colocalized as dot-like structures (Fig. 5C-E). Functionality of VAB-eYFP was confirmed by introducing *pVAB::VAB-sGFP* in *vab* mutants (data not shown). To identify the direct interaction between VAN3 and VAB in vivo, we performed a

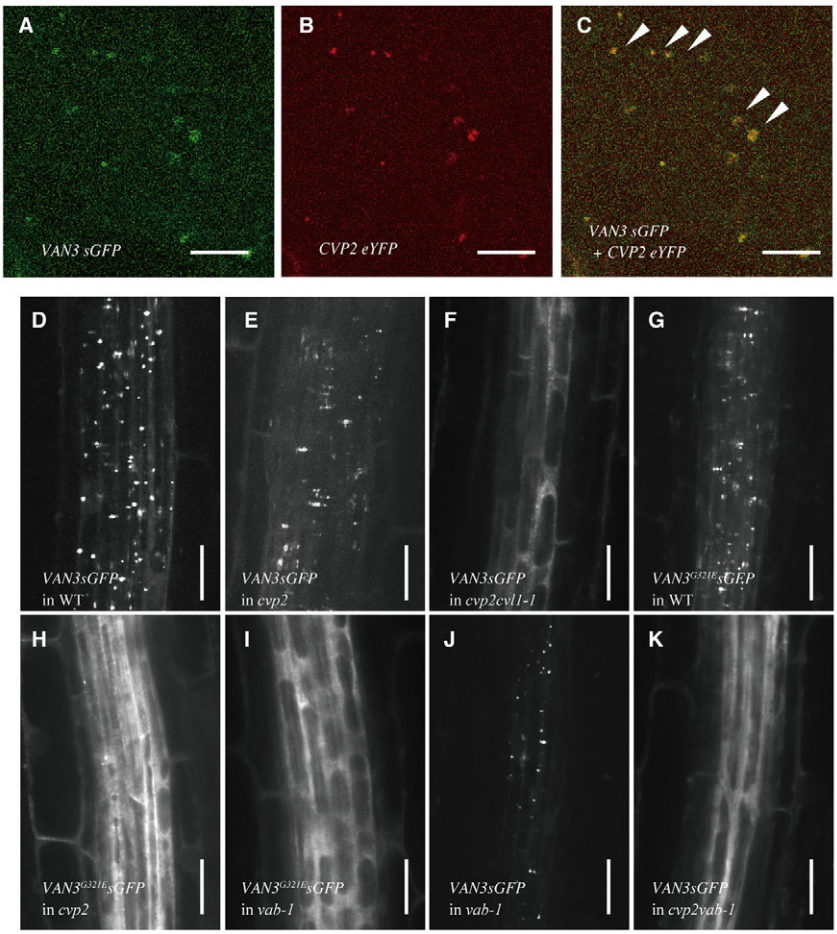

Fig. 4. Interaction of VAN3 with CVP2, CVL1 and VAB. (**A-C**) Subcellular localization of VAN3-sGFP (A), CVP2-eYFP (B) and their merged image (C). (**D-F**) Subcellular localization of VAN3-sGFP in wild-type (D), *cvp2* (E) and *cvp2cvl1* plants (F). (**G-I**) Subcellular localization of VAN3^{G321E}-sGFP in wild-type (G), *cvp2* (H) and *vab* (I) plants. (**J**,**K**) Subcellular localization of VAN3-sGFP in *vab* (J) and *cvp2vab* (K) plants. Scale bars: 10 μm in A-C; 50 μm in D-K.

bimolecular fluorescence complementation (BiFC) analysis (Bracha-Drori et al., 2004; Walter et al., 2004). As a control, we used the VAN3-like 3 (VAL3) protein, which is a member of four plant ACAPs, including VAN3. No YFP fluorescence was detected in *Arabidopsis* protoplasts in which VAB-cYFP (C terminal fragment of YFP) was co-expressed with VAL3-nYFP (N terminal fragment of YFP) (Fig. 5H,I). By contrast, strong dot-like fluorescent signals were observed in protoplasts co-expressing VAN3-nYFP and VAB-cYFP (Fig. 5F,G). This result suggests that VAN3 and VAB form a specific complex in vivo.

To study the involvement of *VAB* in vascular development, we observed the phenotype of *vab* mutants. *vab-1* and *vab-2* mutants caused defects in vascular continuity in cotyledons and leaves: the connection between the midvein and secondary veins, and between the proximal and distal veins, was often lost (Fig. 1I; see Fig. S3D,F in the supplementary material), a pattern that was indistinguishable from the *van3-2* vein pattern (Fig. 1D,I). Although the vein phenotypes were essentially the same between *sfc-9vab-1* and *sfc-9* (see Fig. S3A,C in the supplementary material), veins of both *van3-2vab-1 and van3-2vab-2* mutants were more discontinuous than those in cotyledons (Fig. 1D,I,J; see Fig. S3D,E in the supplementary material) and the first leaves (Fig. 1K-N; see Fig. S3F,G in the supplementary material) of any single mutant. Subsequent PIN1 antibody staining during leaf primodium development revealed that *vab-1* caused a defect in the maintenance of the continuous PIN1 expression cells (see Fig. S4I-L in the supplementary material), and that the abnormal PIN1 expression in *sfc-9* and *sfc-9vab-1* were essentially the same (see Fig. S4M-P,U-X in the supplementary material). These results suggest that VAN3 and VAB function on the pathway at the same point for continuous vein formation, and that VAN3 and VAB may form a complex in a subpopulation of the TGNs to cooperatively regulate the vein continuity.

Because VAB possesses the PH domain and interacts with VAN3, we hypothesized that the VAN3-VAB complex functions in recognizing the PtdIns(4)*P*-enriched domain of the membrane, resulting in the recruitment of VAN3 to the correct membrane domain. To address this issue, we examined the subcellular localization of VAN3 in *vab-1* mutants. The *vab-1* mutation affected the subcellular localization of VAN3^{G321E}-sGFP (Fig. 4I), as did the *cvp2* mutation, although the subcellular localization of VAN3-sGFP did not change dramatically in *vab-1* mutants (Fig. 4J). In addition, the *vab-1* mutation enhanced the mislocation of VAN3-sGFP in the *cvp2* mutant background (Fig. 4K; see Fig. S1D,F in the supplementary material). These results suggest that VAB is involved in the recruitment of VAN3 into the PtdIns(4)*P*-enriched membrane domains of the TGN.

Phosphoinositides-dependent ARF-GAP activity of VAN3

Next, we examined the effect of phospholipids on the ARF-GAP activity of VAN3. To achieve this, GST-tagged VAN3, its derivatives and myristoylated AtARF1 were produced in *E. coli* and purified as shown in the Materials and methods. ARF-GAP activity was quantified using the change in intrinsic Trp fluorescence during the transition from the GTP- to the GDP-bound state of myristoylated

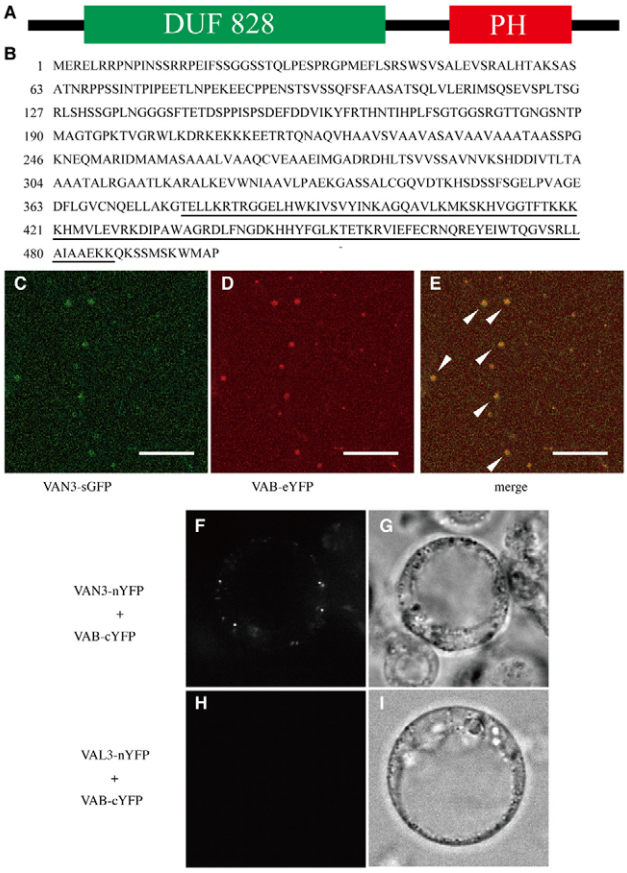

Fig. 5. Molecular characterization of VAB. (**A**) Schematic representation of VAB structure. (**B**) Deduced amino acid sequence of VAB. Underlining indicates the region of the PH domain. (**C-E**) Subcellular localization of VAN3-sGFP (C) and VAB-eYFP (D), and their merged image (E). (**F-I**) BiFC analysis of VAN3 and VAB. (F,G) YFP fluorescence (F) and DIC images (G) of protoplasts co-transformed with VAN3-nYFP and VAB-cYFP. (H,I) YFP fluorescence (H) and DIC images (I) of protoplasts co-transformed with VAL3-nYFP and VAB-cYFP. Scale bars: 10 μm in C-E; 5 μm in F-I.

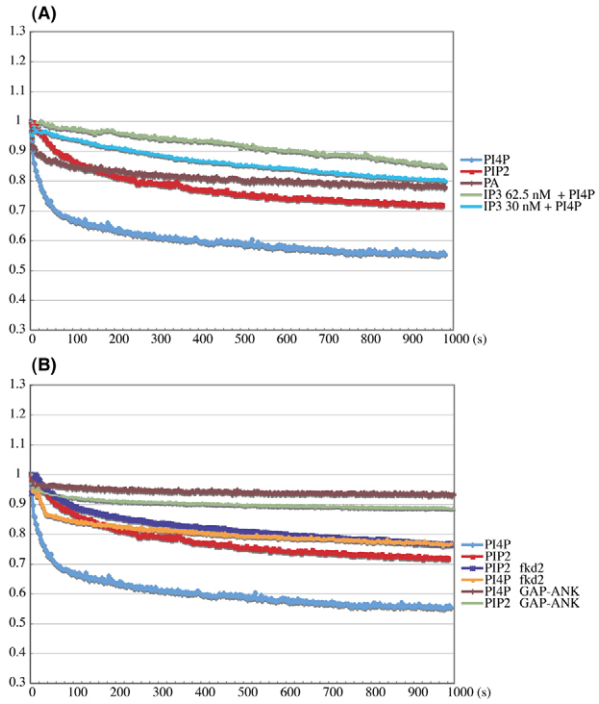

Fig. 6. Effect of phosphoinositides and IP_3 on the ARF-GAP activity of VAN3. VAN3-dependent GTP hydrolysis in myristoylated, GTP-loaded AtArf1 was measured in the presence of phosphoinositides and IP_3. GTP hydrolysis was initiated by the addition of 50 nM of GST-VAN3 and 100 nM of the indicated phosphoinositides, and the nucleotide exchange in the AtArf1 was monitored as the change in autofluorescence of intrinsic tryptophan. (**A**) Phosphoinositide-dependent ARF GAP activity. Different phospholipids or inositol phosphate were added with AtArf1 and VAN3. (**B**) The domain of VAN3 required for ARF GAP activity. Mutated VAN3 proteins were added instead of VAN3.

AtARF1 (Antonny et al., 1997). Although phospholipids such as phosphatidylcholine (PC), phosphatidylserine (PS) and PI have no effects (see Fig. S6A in the supplementary material), the ARF GAP activity of VAN3 was stimulated strongly by PtdIns(4)*P*, and moderately by and PtdIns(4,5)P_2 and phosphatidic acid (PA) (Fig. 6A). By contrast, application of a nonhydrolyzable analogue GMPPNP instead of GTP or application of GST instead of GST-VAN3 did not reduce the fluorescence (see Fig. S6B,C in the supplementary material). These results indicate that the ARF GAP activity of VAN3 is dependent on specific phospholipids and that, among the phospholipids, PtdIns(4)*P* promotes the ARF-GAP activity of VAN3 most efficiently. This finding is consistent with our previous report that the VAN3 PH domain binds to PtdIns(4)*P* more strongly than to other phospholipids (Koizumi et al., 2005).

To examine the requirement of the PH domain for the ARF-GAP activity of VAN3, we constructed a mutant VAN3 protein comprising the ARF-GAP domain and ANK repeats. This truncated VAN3 ($VAN3^{GAP\text{-}ANK}$) had negligible ARF-GAP activity even in the presence of PtdIns(4)*P* or PtdIns(4,5)P_2 (Fig. 6B). In addition, $VAN3^{G321E}$, which harbors the same missense mutation in the PH domain as that of *fkd2/van3-2*, had weaker ARF-GAP activity than the wild-type VAN3 protein (Fig. 6B). These data suggest that binding of PtdIns(4)*P* or PtdIns(4,5)P_2 to the PH domain is indispensable to the ARF-GAP activity of VAN3.

Finally, we examined the effect of IP_3 on ARF-GAP activity of VAN3 because the *CVP2* mutation elevates the level of IP_3 (Carland and Nelson, 2004) and enhances the phenotype of *van3-2*. Addition of IP_3 in the GAP assay solution inhibited the ARF-GAP activity of VAN3 in the presence of PtdIns(4)*P*. The inhibitory effect of IP_3 on the ARF-GAP activity of VAN3 became stronger with higher concentrations of IP_3 (Fig. 6A). This result raises the possibility that CVP2 also upregulates ARF-GAP activity of VAN3 by suppressing the cellular level of IP_3.

DISCUSSION

The PH domain is necessary for TGN localization of VAN3

We demonstrated that VAN3 localize to the TGN. Analysis involving a series of truncated forms of GFP-tagged VAN3 showed that the BAR and PH domains are the minimal requirements for the subcellular localization of VAN3 to the TGN. A mutation in the PH domain of VAN3 resulted in mislocalization of the protein. These

results indicate that the PH domain of VAN3 is necessary for its localization to the TGN. The subcellular localization of animal ACAPs is also determined by both the BAR and the PH domain (Peter et al., 2004). However, any animal ACAP is not localized to the TGN (Jackson et al., 2000; Peter et al., 2004). The differences in subcellular localization between animal and plant ACAPs may relate to differences in binding specificity to phosphatidyl inositols, PtdIns(4)*P* for VAN3 versus PtdIns(4,5)P_2 for animal ACAPs (Jackson et al., 2000). Thole et al. (Thole et al., 2008) recently found using EYFP-FAPP1 as a PtdIns(4)*P* staining agent that PtdIns(4)*P* is localized primarily in the PM but also some internal membranes in *Arabidopsis* root hairs. In addition, PtdIns(4)*P* is produced at the TGN by the PI4Kβ1 in *Arabidopsis* (Preuss et al., 2006). Our results support the presence of PtdIns(4)*P* in the TGN and the PM, and its function in the localization of TGN-residing proteins. In this context, it is interesting that VAN3 is localized in the subdomain of the TGN membrane, which might suggest the presence of the PtdIns(4)*P*-rich subdomain in the TGN membrane. Future EM analysis will be required to prove the existence of PtdIns(4)*P*-rich subdomain in the TGN.

Phosphoinositide signaling functions in the localization of VAN3 to the TGN

In plants, phospholipid signaling regulates a wide variety of phenomena, including pollen germination, regulation of stomata opening and the stress response (Wang, 2004; Xue et al., 2007). Although little is known about the function of phospholipid signaling in venation formation, only 5PTases appear to be involved in this process (Xue et al., 2007). A mutation in *CVP2* encoding a plant type1 5PTase causes weak vascular discontinuity (Carland and Nelson, 2004). A mutation in *At5Pase13* also causes a defect in cotyledon vein formation (Lin et al., 2005). We have identified *van3-2* weak allele mutants, the phenotype of which is enhanced upon introduction of the *CVP2* mutation. In addition, double mutants between *CVP2* and *CVL1* phenocopied the *van3-1* strong allele. We also found that double knockout of *CVP2* and *CVL1* caused mislocalization of VAN3 from the TGN form to the cytosolic form. These results imply that the normal function of VAN3 in the right position is essential for the continuous formation of vascular tissues. In addition, these results suggest that one or more products from CVP2 and CVL1 5PTases are necessary for the correct localization of VAN3.

In animals, type 1-5PTases hydrolyze only soluble inositol phosphates such as IP_3, whereas type 2-5PTases hydrolyze PtdIns(4,5)P_2 and PtdIns(3,4,5)P_3, as well as IP_3 (Majerus et al., 1999). In the *Arabidopsis* genome, at least 15 genes are predicted to encode 5PTases, and these are classified into 11 type 1-like and four type 2-like genes (Berdy et al., 2001). Of the type 2-like PTases, two (AtPTase14 and FRAGILE FIBER3) can hydrolyze PtdIns(4,5)P_2 and PtdIns(3,4,5)P_3, as well as IP_3, and the other two (AtPTase12 and AtPTase13) can hydrolyze only IP_3 (Zhong et al., 2004; Zhong and Ye, 2004). At5PTase1 and At5PTase2, type 1-like 5PTases, exhibit only IP_3-hydrolyzing activity (Berdy et al., 2001; Gunesekera et al., 2007). However, a cooperative mutation in both *At5PTase1* and *At5PTase2* caused both an increase in IP_3 level and a decrease in PtdIns(4)*P* level (Gunesekera et al., 2007). Interestingly, although CVP2 has been classified to the type 1-like 5PTase family, CVP2 has been revealed recently to possess the ability to hydrolyze both IP_3 and PtdIns(4,5)P_2 (Francine M. Carland and Timothy Nelson, personal communication). Therefore, an increase in IP_3 level but also a decrease in PtdIns(4)*P* level is expected to occur in the double knockout mutant of *CVP2* and *CVL1*. Indeed, an increased level of IP_3 was observed in *cvp2* (Carland and Nelson, 2004). Association between the PH domain and the membrane is prompted by some inositol phospholipids and inhibited by some soluble inositols, such as IP_3 (Lemmon and Ferguson, 2000). From these results and the observation that VAN3 binds strongly to PtdIns(4)*P* (Koizumi et al., 2005), we may think that VAN3 is recruited onto the PtdIns(4)*P*-rich subdomain of the TGN by specific binding of its PH domain to PtdIns(4)*P*. IP_3 may suppress the binding. The facts that *AT5PTase13* mutation caused defects in venation continuity and that double mutation of *At5PTase1* and *At5PTase2* caused increase in IP_3 level and a decrease in PtdIns(4)*P* level suggest that not only CVP2/CVL1 but also other 5PTases are also involved in this process. The weaker phenotype of *cvp2cvl1* than that of *sfc-9* is not inconsistent with this notion. Therefore, CVP2 and CVL1, probably together with other 5PTase may contribute to the enhancement of TGN localization of VAN3 (Fig. 7).

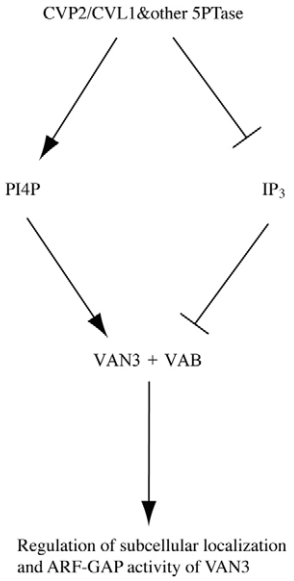

Fig. 7. A model of the 5PTase-mediated VAN3 regulation. At5PTase, including CVP2/CVL1 may increase PtdIns(4)*P* level or decrease IP_3 level or both. PtdIns(4)*P* may have a dual function of recruiting VAN3 to the TGN membranes and promoting the ARF-GAP activity of VAN3, whereas IP_3 may inhibit these processes. This regulation by PtdIns(4)*P* and IP_3 may occur through their association with the PH domain of VAN3. VAB may assist VAN3 in binding to the PtdIns(4)*P*-rich subdomain of the TGN membrane.

VAB is a plant-specific protein containing the PH domain and functions in vascular continuity together with VAN3

Using the yeast two-hybrid system, we identified VAB as a novel VAN3-interacting protein, the homologue of which is not found in animals. The interaction between VAB and VAN3 in situ was strongly supported by (1) colocalization of the two proteins to the TGN, (2) attachment of the two proteins observed with the split YFP and (3) collaboration for vascular continuity demonstrated by genetic analysis. VAB is a plant-specific protein with a PH domain and an unknown domain, DUF828, and forms a small family with the other seven homologues in the *Arabidopsis* genome. The subcellular localization of VAN3^{G321E} was changed in the *vab* mutation background, as did the *cvp2* mutation, suggesting that VAB

is involved in the proper targeting of VAN3. In addition, the *vab* mutation enhanced the mislocation of VAN3-sGFP in the *cvp2* mutant background. Interestingly, VAL1, a VAN3 homologue, was not associated with VAB protein, suggesting the specific binding of VAB with VAN3. It is known that many PH domain-containing proteins have an inherent affinity for the membrane surface that is insufficient by itself to drive their membrane localization, and the formation of a protein complex with other proteins increases the avidity for the membrane, resulting in the membrane recruitment (Lemmon and Ferguson, 2000). This suggests that VAN3 and VAB form a complex to bind to the PtdIns(4)*P*-enriched membrane domain of the TGN, which was also supported by the result of the split-YFP experiment.

PtdIns(4)*P* and IP_3 control both the ARF-GAP activity and the subcellular localization of VAN3

Measurement of ARF-GAP activity indicated that PtdIns(4)*P* enhances and IP_3 inhibits ARF GAP activity of VAN3. This is the first indication of phosphatidylinositol-dependent ARF-GAP activity in plants. In animals, the GAP activity of ASAPs and ACAPs is stimulated by binding of PtdIns(4,5)P_2 and PA to their PH domains (Randazzo, 1997; Brown et al., 1998; Jackson et al., 2000; Kam et al., 2000). However, our results showed the PtdIns(4)*P*-dependent activation of the VAN3 GAP activity. This result is consistent with the specific binding of PtdIns(4)*P* to the VAN3 PH domain (Koizumi et al., 2005). This difference might relate to differences in the subcellular localization between animal ACAPs and VAN3. The accelerating and inhibitory effects on PtdIns(4)*P* and IP_3 for VAN3 ARF-GAP activity, respectively, should be related to the activity of CVP2 (probably and also CVL1), which increase the PtdIns(4)*P* level and decrease the IP_3 level, as discussed above.

Upon these results, we present the model that antagonistic action of PtdIns(4)*P* and IP_3 regulates both the subcellular localization and ARF-GAP activity of VAN3 (Fig. 7). CVP2 and CVL1 contribute to the increase in PtdIns(4)*P* levels and the decrease in IP_3 levels. Both the activity and the localization of VAN3 may be coupled by specific binding of their PH domains to the PtdIns(4)*P*-rich domain in the TGN, and IP_3 may suppress the binding and activation of VAN3. VAB helps VAN3 to bind to PtdIns(4)*P*-enriched membrane domains of the TGN. According to this model, in the *cvp2cvl* mutant, the reduction of PtdIns(4)*P* level on the membranes and an increased level of cellular IP_3 would decrease the affinity of the PH domain of VAN3 for the membrane, resulting in the mislocalization of VAN3, as well as a decrease in ARF GAP activity.

Molecular function of VAN3 in continuous formation of vascular tissues

In conclusion, our findings strongly suggest that phosphoinositide signaling plays a pivotal role in continuous vascular formation by regulating the subcellular localization and ARF-GAP activity of VAN3. Polar auxin transport is an essential factor that induces vascular pattern formation (Sachs, 1981; Scarpella et al., 2006). Sachs (Sachs, 1981) proposed the 'auxin signal flow canalization hypothesis': auxin flow, starting initially with diffusion, induces the formation of the polar auxin transport cell system. This, in turn, promotes auxin transport and leads to canalization of the auxin flow along a narrow file of cells. This continuous file of cells differentiates into a strand of vascular cells. According to this hypothesis, the positive-feedback system of auxin transport is a key event, but its mechanism is still mysterious. This hypothesis agrees with accumulating data on PIN proteins (Benková et al., 2003). In the *sfc* root, the treatment with brefeldin A results in the accumulation of PIN1, an auxin efflux carrier, in smaller and more numerous compartments than in the wild type (Sieburth et al., 2006). This suggests that VAN3/SFC may be involved in PIN1 targeting. Conversely, a recent report shows that auxin regulates phosphoinositide signaling (Xue et al., 2007). Therefore, it is possible that auxin promotes VAN3 function through CVP2-mediated phosphoinositide signaling, and, in turn, that VAN3 promotes auxin transport through the polar localization of PIN proteins to establish the vascular continuity. We are currently investigating this hypothesis.

We thank the ABRC for seeds of Salk T-DNA lines, CAMBIA for pCAMBIA vectors, Taku Demura for pHGY and Tsuyoshi Nakagawa for pGWB2 vectors. We thank Elizabeth Schultz and Timothy Nelson for seeds of the *fkd2* and *cvp2*, respectively. We also thank Tatsuaki Goh, Minoru Nagano and Yuki Yanagawa for the support of our experiment and Atsushi Miyawaki for the VENUS construct. This work was supported in part by Grants-in-Aid from the Japan Society for the Promotion of Science (to S.N., 20247003 to H.F.), Scientific Research for Plant Graduate Student from Nara Institute of Science and Technology, Supported by The Ministry of Education, Culture, Sports, Science and Technology, Japan (to S.N.), MEXT, Japan (19060009 to H.F.), and the Program of Basic Research Activities for Innovative Biosciences from BRAIN (to H.F.).

Supplementary material

Supplementary material for this article is available at
http://dev.biologists.org/cgi/content/full/136/9/1529/DC1

References

Antonny, B., Beraud-Dufour, S., Chardin, P. and Chabre, M. (1997). N-terminal hydrophobic residues of the G-protein ADP-ribosylation factor-1 insert into membrane phospholipids upon GDP to GTP exchange. *Biochemistry* **36**, 4675-4684.

Benková, E., Michniewicz, M., Sauer, M., Teichmann, T., Seifertová, D., Jürgens, G. and Friml, J. (2003). Local, efflux-dependent auxin gradients as a common module for plant organ formation. *Cell* **115**, 591-602.

Berdy, S. E., Kudla, J., Gruissem, W. and Gillaspy, G. E. (2001). Molecular characterization of At5PTase1, an inositol phosphatase capable of terminating inositol trisphosphate signaling. *Plant Physiol.* **126**, 801-810.

Bracha-Drori, K., Shichrur, K., Katz, A., Oliva, M., Angelovici, R., Yalovsky, S. and Ohad, N. (2004). Detection of protein-protein interactions in plants using bimolecular fluorescence complementation. *Plant J.* **40**, 419-427.

Brown, M. T., Andrade, J., Radhakrishna, H., Donaldson, J. G., Cooper, J. A. and Randazzo, P. A. (1998). ASAP1, a phospholipid-dependent arf GTPase-activating protein that associates with and is phosphorylated by Src. *Mol. Cell. Biol.* **18**, 7038-7051.

Carland, F. M. and Nelson, T. (2004). Cotyledon Vascular Pattern2-mediated inositol (1,4,5) triphosphate signal transduotion is essential for closed venation patterns of Arabidolpsis foliar organs. *Plant Cell* **16**, 1263-1275.

Carland, F. M., Berg, B. L., FitzGerald, J. N., Jinamornphongs, S., Nelson, T. and Keith, B. (1999). Genetic regulation of vascular tissue patterning in Arabidopsis. *Plant Cell* **11**, 2123-2137.

Deyholos, M. K., Cordner, G., Beebe, D. and Sieburth, L. E. (2000). The SCARFACE gene is required for cotyledon and leaf vein patterning. *Development* **127**, 3205-3213.

Donaldson, J. G. and Klausner, R. D. (1994). ARF: a key regulatory switch in membrane traffic and organelle structure. *Curr. Opin. Cell Biol.* **6**, 527-532.

Friml, J., Benkova, E., Mayer, U., Palme, K. and Muster, G. (2003). Automated whole mount localisation techniques for plant seedlings. *Plant. J.* **34**, 115-124.

Geldner, N., Friml, J., Stierhof, Y. D., Jürgens, G. and Palme, K. (2001). Auxin transport inhibitors block PIN1 cycling and vesicle trafficking. *Nature* **413**, 425-428.

Geldner, N., Anders, N., Wolters, H., Keicher, J., Kornberger, W., Muller, P., Delbarre, A., Ueda, T., Nakano, A. and Jürgens, G. (2003). The Arabidopsis GNOM ARF-GEF mediates endosomal recycling, auxin transport, and auxin-dependent plant growth. *Cell* **112**, 219-230.

Goh, T., Uchida, W., Arakawa, S., Ito, E., Dainobu, T., Ebine, K., Takeuchi, M., Sato, K., Ueda, T. and Nakano, A. (2007). VPS9a, the common activator for two distinct types of Rab5 GTPases, is essential for the development of Arabidopsis thaliana. *Plant Cell* **19**, 3504-3515.

Gunesekera, B., Torabinejad, J., Robinson, J. and Gillaspy, G. E. (2007). Inositol polyphosphate 5-phosphatases 1 and 2 are required for regulating seedling growth. *Plant Physiol.* **143**, 1408-1417.

Hardtke, C. S. and Berleth, T. (1998). The Arabidopsis gene MONOPTEROS encodes a transcription factor mediating embryo axis formation and vascular development. *EMBO J.* **17**, 1405-1411.

Jackson, T. R., Brown, F. D., Nie, Z., Miura, K., Foroni, L., Sun, J., Hsu, V. W., Donaldson, J. G. and Randazzo, P. A. (2000). ACAPs are arf6 GTPase-activating proteins that function in the cell periphery. *J. Cell Biol.* **151**, 627-638.
Kam, J. L., Miura, K., Jackson, T. R., Gruschus, J., Roller, P., Stauffer, S., Clark, J., Aneja, R. and Randazzo, P. A. (2000). Phosphoinositide-dependent activation of the ADP-ribosylation factor GTPase-activating protein ASAP1. Evidence for the pleckstrin homology domain functioning as an allosteric site. *J. Biol. Chem.* **275**, 9653-9663.
Koizumi, K., Sugiyama, M. and Fukuda, H. (2000). A series of novel mutants of Arabidopsis thaliana that are defective in the formation of continuous vascular network: calling the auxin signal flow canalization hypothesis into question. *Development* **127**, 3197-3204.
Koizumi, K., Naramoto, S., Sawa, S., Yahara, N., Ueda, T., Nakano, A., Sugiyama, M. and Fukuda, H. (2005). VAN3 ARF-GAP-mediated vesicle transport is involved in leaf vascular network formation. *Development* **132**, 1699-1711.
Kubo, M., Udagawa, M., Nishikubo, N., Horiguchi, G., Yamaguchi, M., Ito, J., Mimura, T., Fukuda, H. and Demura, T. (2005). Transcription switches for protoxylem and metaxylem vessel formation. *Genes Dev.* **19**, 1855-1860.
Lemmon, M. A. and Ferguson, K. M. (2000). Signal-dependent membrane targeting by pleckstrin homology (PH) domains. *Biochem. J.* **350**, 1-18.
Li, J., Ballif, B. A., Powelka, A. M., Dai, J., Gygi, S. P. and Hsu, V. W. (2005). Phosphorylation of ACAP1 by Akt regulates the stimulation-dependent recycling of integrin beta1 to control cell migration. *Dev. Cell* **9**, 663-673.
Lin, W. H., Wang, Y., Mueller-Roeber, B., Brearley, C. A., Xu, Z. H. and Xue, H. W. (2005). At5PTase13 modulates cotyledon vein development through regulating auxin homeostasis. *Plant Physiol.* **139**, 1677-1691.
Majerus, P. W., Kisseleva, M. V. and Norris, F. A. (1999). The role of phosphatases in inositol signaling reactions. *J. Biol. Chem.* **274**, 10669-10672.
Mattsson, J., Sung, Z. R. and Berleth, T. (1999). Responses of plant vascular systems to auxin transport inhibition. *Development* **126**, 2979-2991.
Miura, K., Jacques, K. M., Stauffer, S., Kubosaki, A., Zhu, K., Hirsch, D. S., Resau, J., Zheng, Y. and Randazzo, P. A. (2002). ARAP1: a point of convergence for Arf and Rho signaling. *Mol. Cell* **9**, 109-119.
Moss, J. and Vaughan, M. (1995). Structure and function of ARF proteins: activators of cholera toxin and critical components of intracellular vesicular transport processes. *J. Biol. Chem.* **270**, 12327-12330.
Moss, J. and Vaughan, M. (1998). Molecules in the ARF orbit. *J. Biol. Chem.* **273**, 21431-21434.
Motose, H., Sugiyama, M. and Fukuda, H. (2004). A proteoglycan mediates inductive interaction during plant vascular development. *Nature* **429**, 873-878.
Nagai, T., Ibata, K., Park, E. S., Kubota, M., Mikoshiba, K. and Miyawaki, A. (2002). A variant of yellow fluorescent protein with fast and efficient maturation for cell-biological applications. *Nat. Biotechnol.* **20**, 87-90.
Nakagawa, T., Kurose, T., Hino, T., Tanaka, K., Kawamukai, M., Niwa, Y., Toyooka, K., Matsuoka, K., Jinbo, T. and Kimura, T. (2007). Development of series of gateway binary vectors, pGWBs, for realizing efficient construction of fusion genes for plant transformation. *J. Biosci. Bioeng.* **104**, 34-41.
Nie, Z., Boehm, M., Boja, E. S., Vass, W. C., Bonifacino, J. S., Fales, H. M. and Randazzo, P. A. (2003). Specific regulation of the adaptor protein complex AP-3 by the Arf GAP AGAP1. *Dev. Cell* **5**, 513-521.
Niwa, Y., Hirano, T., Yoshimoto, K., Shimizu, M. and Kobayashi, H. (1999). Non-invasive quantitative detection and applications of non-toxic, S65T-type green fluorescent protein in living plants. *Plant J.* **18**, 455-463.
Paciorek, T., Zažímalová, E., Ruthardt, N., Petrášek, J., Stierhof, Y. D., Kleine-Vehn, J., Morris, D. A., Emans, N., Jürgens, G., Geldner, N. et al. (2005). Auxin inhibits endocytosis and promotes its own efflux from cells. *Nature* **435**, 1251-1256.
Peter, B. J., Kent, H. M., Mills, I. G., Vallis, Y., Butler, P. J., Evans, P. R. and McMahon, H. T. (2004). BAR domains as sensors of membrane curvature: the amphiphysin BAR structure. *Science* **303**, 495-499.
Preuss, M. L., Schmitz, A. J., Thole, J. M., Bonner, H. K., Otegui, M. S. and Nielsen, E. (2006). A role for the RabA4b effector protein PI-4Kbeta1 in polarized expansion of root hair cells in Arabidopsis thaliana. *J. Cell Biol.* **172**, 991-998.
Przemeck, G. K. H., Mattsson, J., Hardtke, C. S., Sung, Z. R. and Berleth, T. (1996). Studies on the role of the Arabidopsis gene MONOPTEROS in vascular development and plant cell axialization. *Planta* **200**, 229-237.
Randazzo, P. A. (1997). Resolution of two ADP-ribosylation factor 1 GTPase-activating proteins from rat liver. *Biochem. J.* **324**, 413-419.
Randazzo, P. A. and Hirsch, D. S. (2004). Arf GAPs: multifunctional proteins that regulate membrane traffic and actin remodelling. *Cell Signal.* **16**, 401-413.
Randazzo, P. A., Andrade, J., Miura, K., Brown, M. T., Long, Y. Q., Stauffer, S., Roller, P. and Cooper, J. A. (2000). The Arf GTPase-activating protein ASAP1 regulates the actin cytoskeleton. *Proc. Natl. Acad. Sci. USA* **97**, 4011-4016.
Sachs, T. (1981). The control of patterned differentiation of vascular tissues. *Adv. Bot. Res.* **9**, 152-262.
Sakai, T., Honing, H., Nishioka, M., Uehara, Y., Takahashi, M., Fujisawa, N., Saji, K., Seki, M., Shinozaki, K., Jones, M. A. et al. (2008). Armadillo repeat-containing kinesins and a NIMA-related kinase are required for epidermal-cell morphogenesis in Arabidopsis. *Plant J.* **53**, 157-171.
Sawa, S., Koizumi, K., Naramoto, S., Demura, T., Ueda, T., Nakano, A. and Fukuda, H. (2005). DRP1A is responsible for vascular continuity synergistically working with VAN3 in Arabidopsis. *Plant Physiol.* **138**, 819-826.
Scarpella, E., Marcos, D., Friml, J. and Berleth, T. (2006). Control of leaf vascular patterning by polar auxin transport. *Genes Dev.* **20**, 1015-1027.
Sieburth, L. E., Muday, G. K., King, E. J., Benton, G., Kim, S., Metcalf, K. E., Meyers, L., Seamen, E. and Van Norman, J. M. (2006). SCARFACE encodes an ARF-GAP that is required for normal auxin efflux and vein patterning in Arabidopsis. *Plant Cell* **18**, 1396-1411.
Steynen, Q. J. and Schultz, E. A. (2003). The FORKED genes are essential for distal vein meeting in Arabidopsis. *Development* **130**, 4695-4708.
Thole, J. M., Vermeer, J. E., Zhang, Y., Gadella, T. W., Jr and Nielsen, E. (2008). Root hair defective4 encodes a phosphatidylinositol-4-phosphate phosphatase required for proper root hair development in Arabidopsis thaliana. *Plant Cell* **20**, 381-395.
Tian, G. W., Mohanty, A., Chary, S. N., Li, S., Paap, B., Drakakaki, G., Kopec, C. D., Li, J., Ehrhardt, D., Jackson, D. et al. (2004). High-throughput fluorescent tagging of full-length Arabidopsis gene products in planta. *Plant Physiol.* **135**, 25-38.
Uemura, T., Ueda, T., Ohniwa, R. L., Nakano, A., Takeyasu, K. and Sato, M. H. (2004). Systematic analysis of SNARE molecules in Arabidopsis: dissection of the post-Golgi network in plant cells. *Cell Struct. Funct.* **29**, 49-65.
Walter, M., Chaban, C., Schutze, K., Batistic, O., Weckermann, K., Nake, C., Blazevic, D., Grefen, C., Schumacher, K., Oecking, C. et al. (2004). Visualization of protein interactions in living plant cells using bimolecular fluorescence complementation. *Plant J.* **40**, 428-438.
Wang, X. (2004). Lipid signaling. *Curr. Opin. Plant Biol.* **7**, 329-336.
Wee, E. G., Sherrier, D. J., Prime, T. A. and Dupree, P. (1998). Targeting of active sialyltransferase to the plant Golgi apparatus. *Plant Cell* **10**, 1759-1768.
Wisniewska, J., Xu, J., Seifertová, D., Brewer, P. B., Ruzicka, K., Blilou, I., Rouquié, D., Benková, E., Scheres, B. and Friml, J. (2006). Polar PIN localization directs auxin flow in plants. *Science* **312**, 883.
Xue, H., Chen, X. and Li, G. (2007). Involvement of phospholipid signaling in plant growth and hormone effects. *Curr. Opin. Plant Biol.* **10**, 483-489.
Zhong, R. and Ye, Z. H. (2004). Molecular and biochemical characterization of three WD-repeat-domain-containing inositol polyphosphate 5-phosphatases in Arabidopsis thaliana. *Plant Cell Physiol.* **45**, 1720-1728.
Zhong, R., Burk, D. H., Morrison, W. H., 3rd and Ye, Z. H. (2004). FRAGILE FIBER3, an Arabidopsis gene encoding a type II inositol polyphosphate 5-phosphatase, is required for secondary wall synthesis and actin organization in fiber cells. *Plant Cell* **16**, 3242-3259.

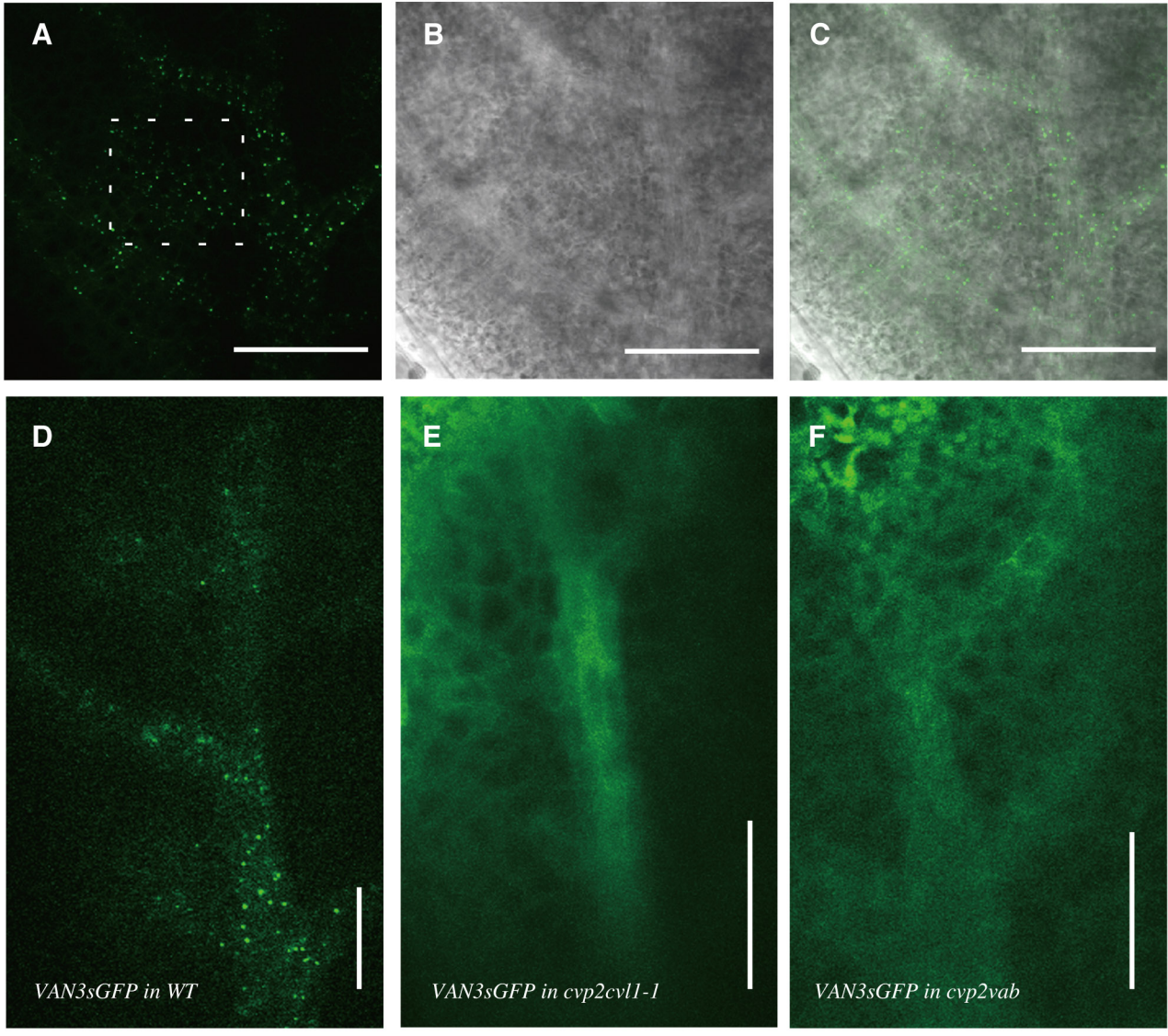
A
B
C
D
E
F
VAN3sGFP in WT
VAN3sGFP in cvp2cvl1-1
VAN3sGFP in cvp2vab

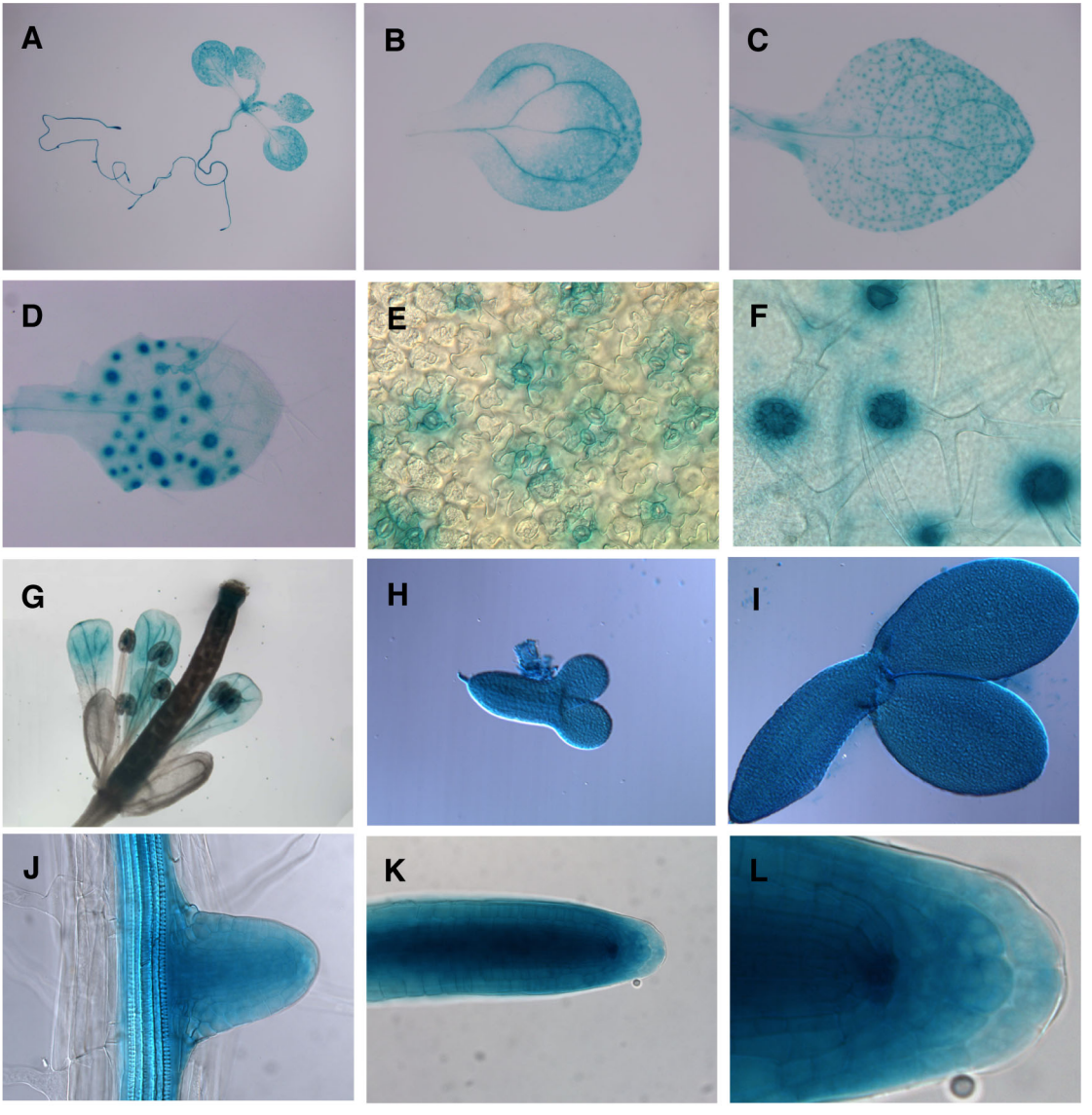
A
B
C
D
E
F
G
H
I
J
K
L

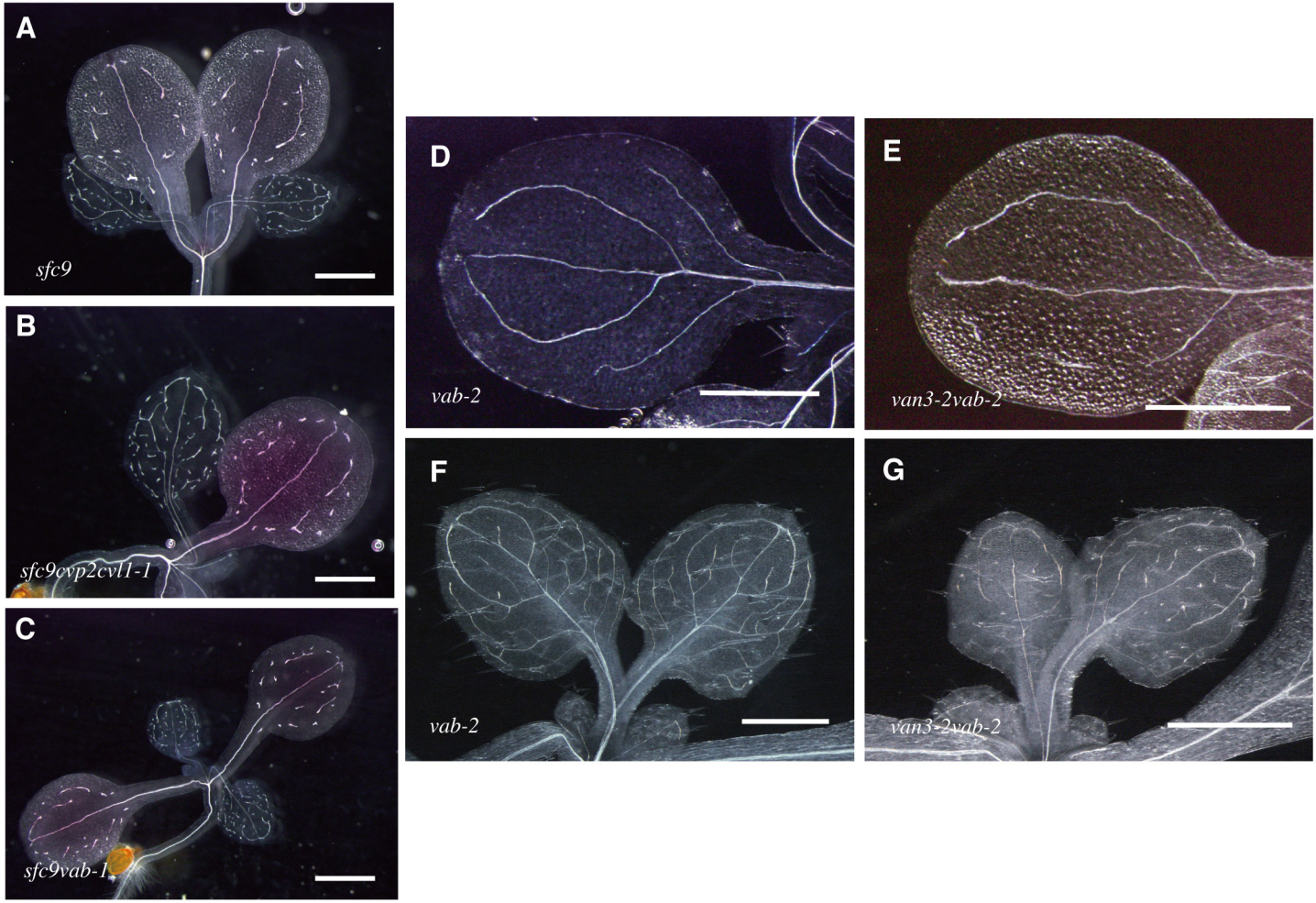
A
sfc9
B
sfc9cvp2cvl1-1
C
sfc9vab-1
D
vab-2
E
van3-2vab-2
F
vab-2
G
van3-2vab-2

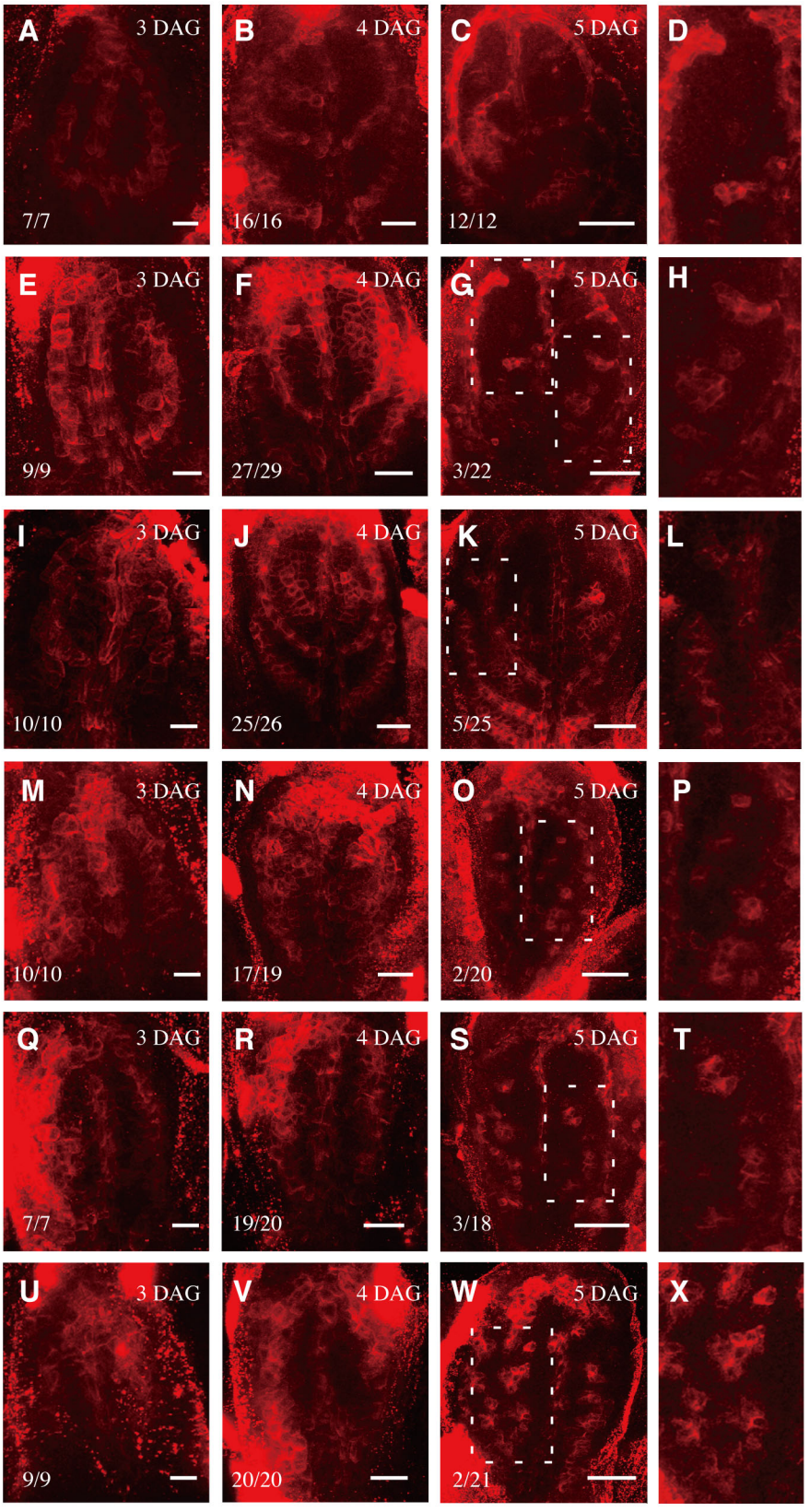
A
3 DAG
7/7
B
4 DAG
16/16
C
5 DAG
12/12
D
E
3 DAG
9/9
F
4 DAG
27/29
G
5 DAG
3/22
H
I
3 DAG
10/10
J
4 DAG
25/26
K
5 DAG
5/25
L
M
3 DAG
10/10
N
4 DAG
17/19
O
5 DAG
2/20
P
Q
3 DAG
7/7
R
4 DAG
19/20
S
5 DAG
3/18
T
U
3 DAG
9/9
V
4 DAG
20/20
W
5 DAG
2/21
X

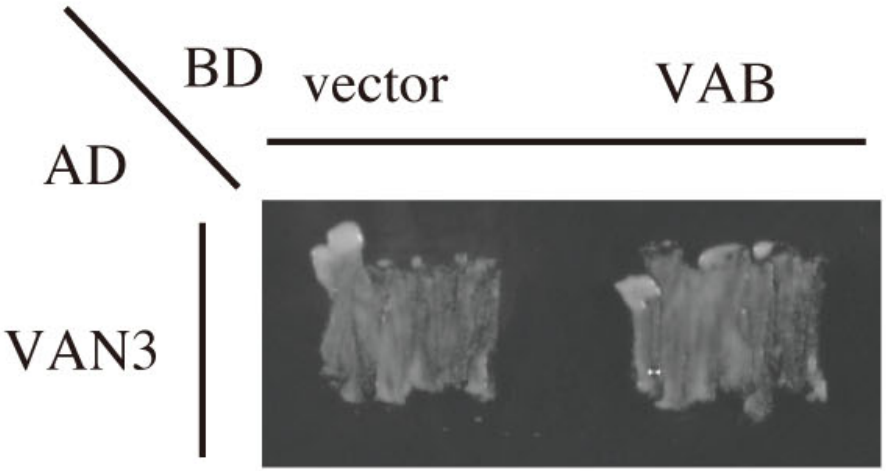
BD
vector
VAB
AD
VAN3

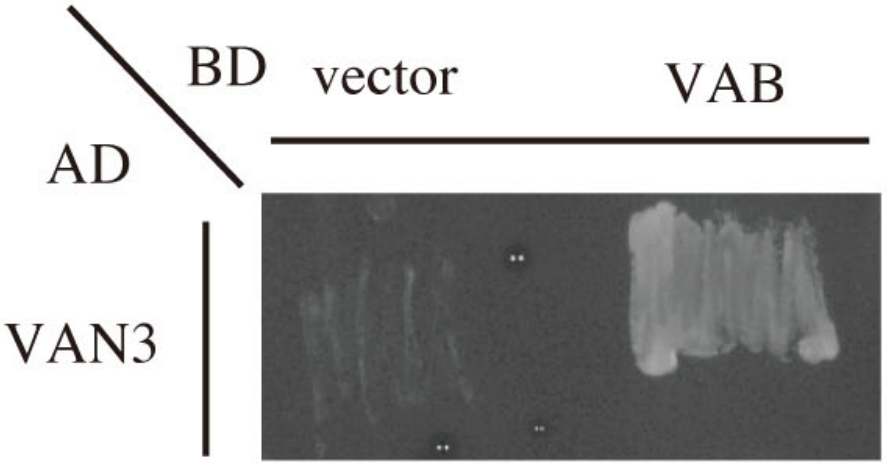
BD
vector
VAB
AD
VAN3

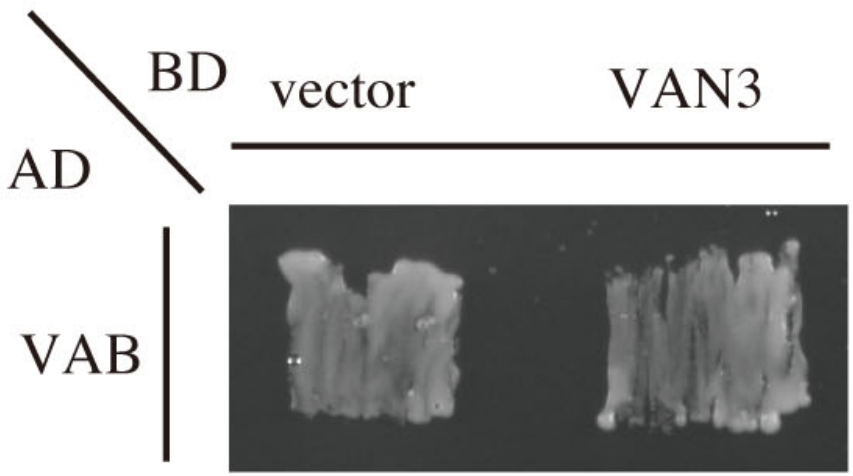
BD
vector
VAN3
AD
VAB

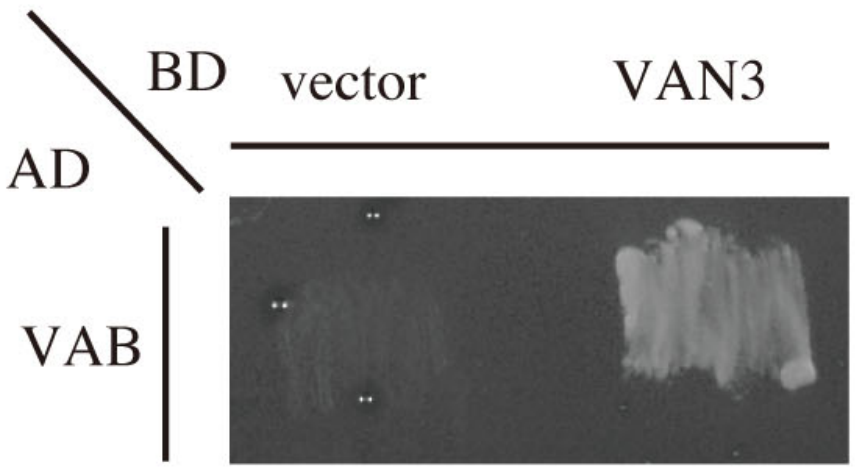
BD
vector
VAN3
AD
VAB

+ HIS

- HIS

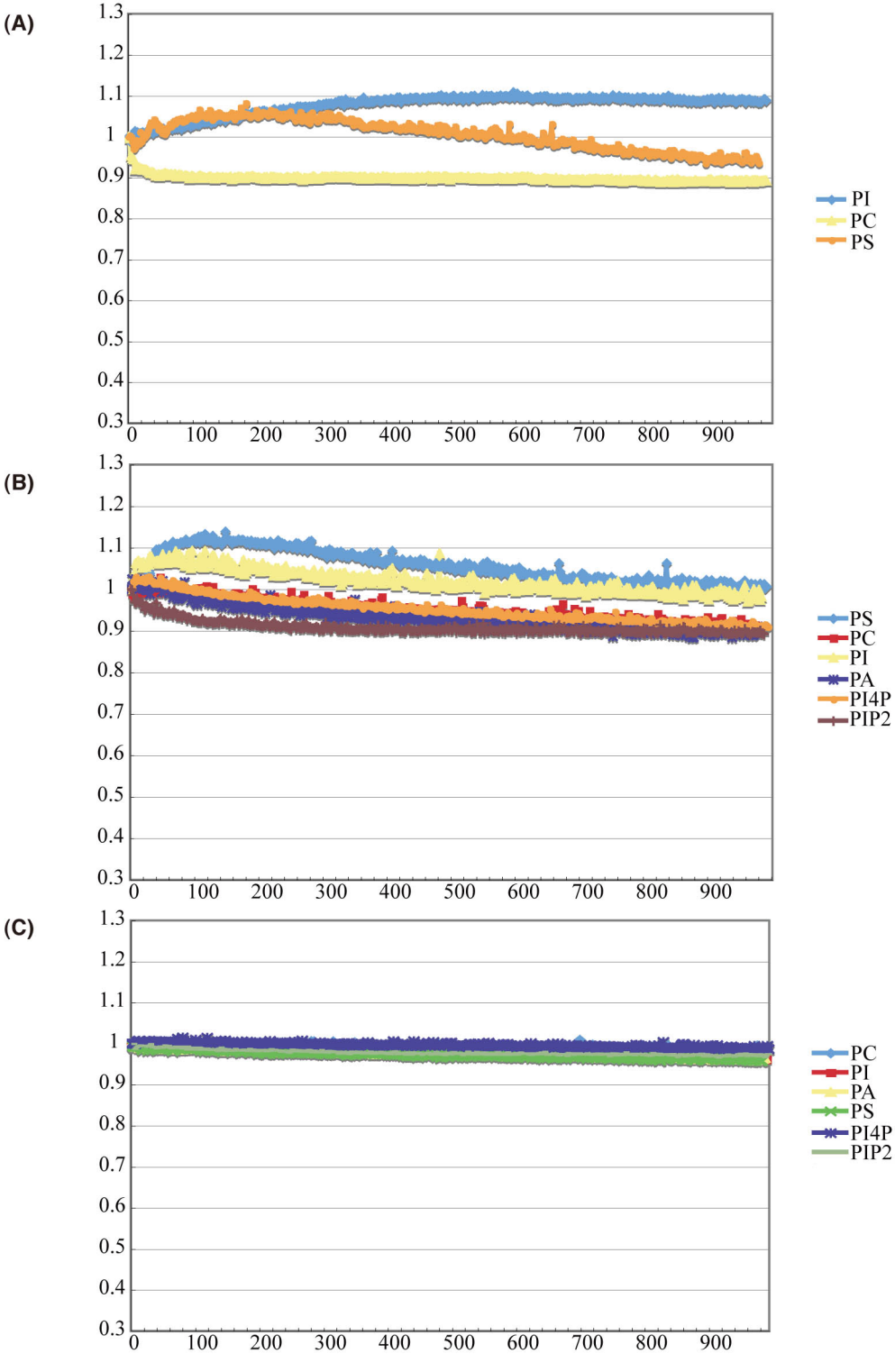
(A)
1.3
1.2
1.1
1
0.9
0.8
0.7
0.6
0.5
0.4
0.3
0
100
200
300
400
500
600
700
800
900
PI
PC
PS
(B)
1.3
1.2
1.1
1
0.9
0.8
0.7
0.6
0.5
0.4
0.3
0
100
200
300
400
500
600
700
800
900
PS
PC
PI
PA
PI4P
PIP2
(C)
1.3
1.2
1.1
1
0.9
0.8
0.7
0.6
0.5
0.4
0.3
0
100
200
300
400
500
600
700
800
900
PC
PI
PA
PS
PI4P
PIP2